Response of externally excited coaxial cables with wire braided shields

Dr S Sali , Bsc , PhD
Department of Electrical and Electronic Engineering
Merz Court, The University of Newcastle, Newcastle upon Tyne NE1 7RU, United Kingdom

ABSTRACT

The frequency responses of coaxial cables employing wire braided shields, excited by external fields is studied using an algorithm based on distributed circuit model, which uses both electric and magnetic field parameters to model the external field coupling. Simplicity and fast speed of the model enable computer aided analysis of externally induced noise in cable interconnects to be carried out in a computationally efficient manner. A general CAD algorithm is developed based on this model and it is applied to study the response of cables over a lossless ground plane. The algorithm is then used to study the effects of different braid constructions on the responses of cables excited by external fields. Responses of cables with optimum braid designs in their shields are studied in detail. The model uses the experimental values of the leakage parameters which are measured separately using a standard triaxial text fixture.

INTRODUCTION

With the advent of smaller and denser integrated circuits very large electronic systems have resulted and these require very complex networks of interconnections within a limited space [Bayindir and Sali, 1990][Sali 1993]. Coaxial cables are used as signal carriers in such interconnection networks between the equipments when extra shielding against the external interfering fields is required. Since the interconnect cables have to be mechanically flexible usually braided coaxial cables are used as signal carriers. Price paid for the flexibility is a conducting shield with a large number of small diamond shaped holes [Sali 1993][Vance 1973] caused by the braiding of the shield wires. Such shields therefore do not provide complete immunity against external interfering fields, which may penetrate inside the cable. The mechanisms of wave penetration are directly related to the geometry of the braid and the frequency of the incident field [Sali, 1990]. At radio frequencies the coupling of the external magnetic field is governed by the Transfer Impedance (Z_T) per-unit-length and the coupling of the external Electric field is governed by Transfer Admittance (Y_T) per-unit-length . A detailed experimental and theoretical study on both parameters are given in [Fowler 1979]. These studies have already demonstrated that Z_T is purely inductive and Y_T is purely capacitive at frequencies above 2 MHz.

Inductive rise of Z_T at high frequencies is caused by two magnetic coupling process : the coupling by direct penetration of external fields to the interior through the holes in the shield which gives rise to hole inductance, and the magnetic flux coupling in the circuits between the inner and outer braid layers of the braid which results in braid inductance. It is known that [Tyni 1976] for braid angles less than 45^0 hole and braid inductances oppose each other and greatly reduced transfer impedance values may be obtained for certain braid constructions where the difference between the two is minimum and such braid designs are called optimum.

The objective of the work reported here is to develop a general algorithm for the computation of transmission line currents and voltages induced by the external field of arbitrary incidence at any point along the interior of the coaxial cable, placed over a finite-loss conducting plane. The model uses both Y_T and Z_T in contrast to earlier studies which ignores Y_T and hence do not applicable to optimised cables.

A large number of simulations have been carried out to illustrate the capability of the new algorithm. The effects of the high and low value passive load impedances on the amount of coupling are investigated in detail. The effect of polarisation of the incident wave on the coupling of the external field is studied against the angular orientation of the cable with respect to the direction of incidence.

BASIC MODEL FOR INTERFERENCE AND THE LINE RESPONSE

The basic interference model studied is shown in Fig.1, which shows a braided coaxial cable of length **L** ,placed over a finite-loss conducting plane at a height of **h**. The line is illuminated by an external electromagnetic plane wave at an elevation angle of θ and azimuth angle ϕ. Cross dimensions of the coaxial cable and its separation from the conducting plane is much smaller than the wavelength of the illuminating wave and hence the principal mode of propagation in the coax is **TEM.** The electric and magnetic field components of the incident wave couples to the exterior circuit between the shield and the metallic ground plane, inducing electric and magnetic flux there, as shown in Fig.2. This flux coupling is represented in terms of impressed sources $e(\upsilon)$ and $i(\upsilon)$ and per-unit-length equivalent circuit shown in Fig.3 is

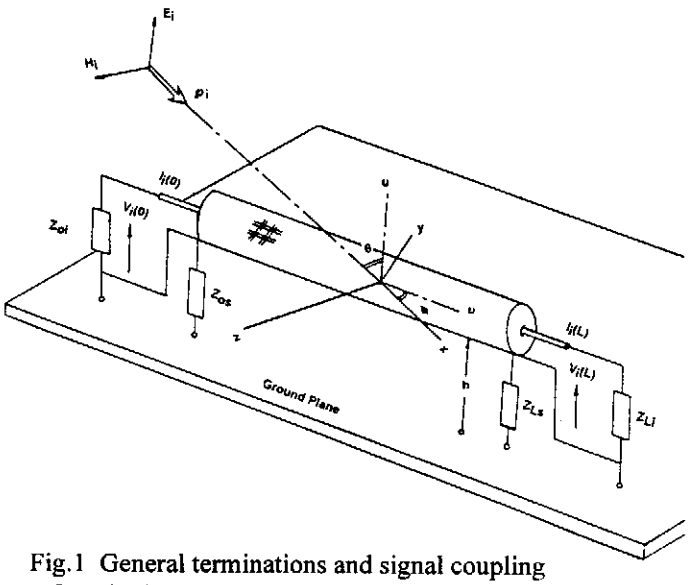

Fig.1 General terminations and signal coupling for a braided coaxial cable over a finite loss conducting plane excited by a plane wave.

employed for the interference problem shown in Fig.1. It is assumed that the tertiary circuit is terminated in passive impedances Z_{0s} at the near end and Z_{Ls} at the far end respectively.

The propagation of the coupled wave in the tertiary circuit is characterised by the propagation constant $\gamma_s = \sqrt{Y_s Z_s}$, and the characteristic impedance $Z_{cs} = \sqrt{Z_s/Y_s}$. Using the method developed in [Sali, 1993] the coupled voltage and current in the teriary are given by

$$V_s(\upsilon) = \cosh \gamma_s \upsilon V_s + Z_{cs} \sinh \gamma_s \upsilon \, I_s(0) + \vartheta_{ss}(\upsilon)$$

$$I_s(\upsilon) = \frac{1}{Z_{cs}} \sinh \gamma_s \upsilon \, V_s(0) + \cosh \gamma_s \upsilon \, I_s(0) + \delta_{ss}(\upsilon) \qquad (1)$$

$$\vartheta_{ss}(\upsilon) = \int_0^{\upsilon} \cosh\gamma_s(\upsilon-\zeta) e_s(\upsilon) d\zeta$$

$$- Z_{cs} \int_0^{\upsilon} \sinh\gamma_s(\upsilon-\zeta) i_s(\zeta) d\zeta \qquad (2)$$

$$\delta_{ss}(\upsilon) = - \frac{1}{Z_{cs}} \int_0^{\upsilon} \sinh\gamma_s(\upsilon-\zeta) e(\zeta) d\zeta$$

$$+ \int_0^{\upsilon} \cosh\gamma_s(\upsilon-\zeta) i_s(\zeta) d\zeta \qquad (3)$$

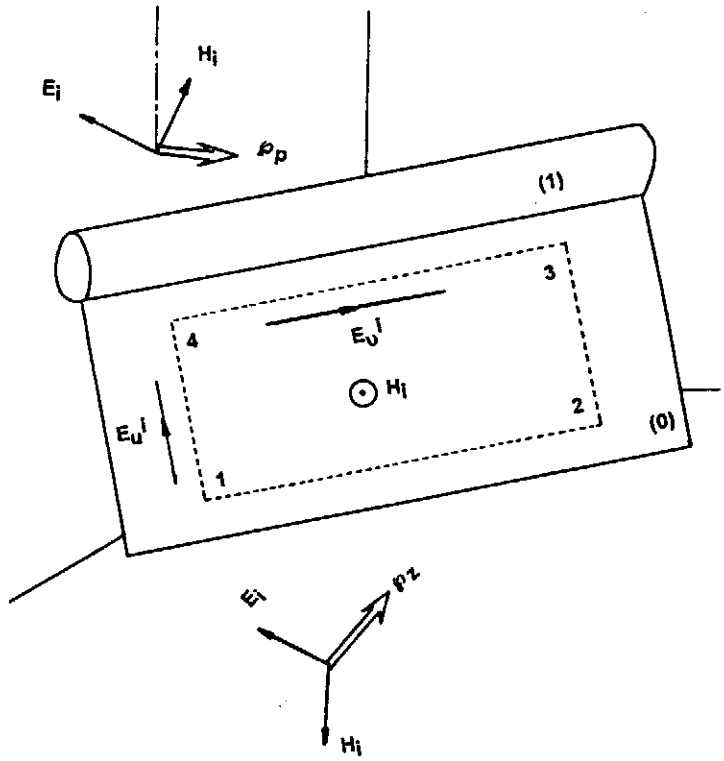

Fig.2 Geometry and contour integration for the calculation of the coupled sources induced by the plane wave.

$$e_s(\upsilon) = [E_\upsilon^i(h,\upsilon) - E_\upsilon^i(0,\upsilon)] - \int_0^h \frac{\partial E_u^i(u,\upsilon)}{\partial \upsilon} du$$

$$i_s(\upsilon) = Y_s \int_0^h E_u^i(u,\upsilon) \, du \qquad (4)$$

The current and voltage in (1) now couple to the interior of the coaxial line giving rise to a TEM wave propagating inside. This wave coupling process is governed by the per-unit-length sources which are described as

$$e_{Ti}(\upsilon) = Z_T I_S(\upsilon) \qquad (5)$$

$$i_{Ti}(\upsilon) = Y_T V_S(\upsilon) \qquad (6)$$

Using the similar process as above the coupled current and voltage inside the coaxial cable are given by

$$V_i(\upsilon)=\cosh\gamma_i\upsilon V_i(0)$$

$$- Z_{ci}\sinh\gamma_i\upsilon I_i(\upsilon) + \vartheta_{si}(\upsilon)$$

$$I_i(\upsilon) = -\frac{1}{Z_{ci}}\sinh\gamma_i\upsilon V_i(0) + \cosh\gamma_i\upsilon I_i(0) + \delta_{si}(\upsilon) \qquad (7)$$

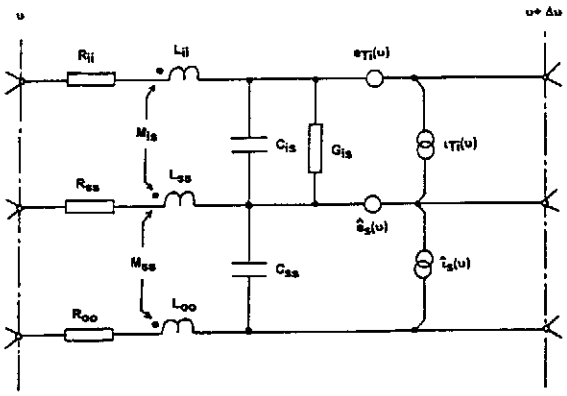

Fig.3 The per-unit-length equivalent circuit for the coaxial cable in Fig. 1

Since defining the field coupling in terms circuit parameters Y_T and Z_T isolates the two TEM waves inside and outside the coaxial cable the transmission line equations in (1) and (7) are independent. This allows the boundary conditions to be considered separately in terms of the passive terminations at both ends of each circuit. These are given by the Thevenin equations as $V_{s,i}(0) = - Z_{os,i}\, I_{s,i}(0)$ $V_{s,i} = Z_{Ls,i} I_{s,i}(L)$ Inserting these boundary conditions in (1) and (7) the equivalent distributed sources inside the coaxial cable becomes

$$\vartheta_{si}(\upsilon)= \frac{Z_T}{Z_{cs}}\frac{\kappa_{ss}}{\Delta_{ss}}\int_0^{\upsilon} \cosh\gamma_i(\upsilon-\varsigma)\, X$$

$$(Z_{os}\sinh\gamma_s\zeta+\cosh\gamma_s\zeta)d\zeta$$

$$-\int_0^{\upsilon} \cosh\gamma i(\upsilon-\upsilon)\{\eta(0)\sinh\gamma s\upsilon$$

$$+\int_0^{\upsilon} \sinh\gamma_s(\upsilon-\varsigma)\tau(\varsigma)d\varsigma\}d\upsilon$$

$$+ Z_{ci}Y_T\int_0^{\upsilon} \sinh\gamma_i(\upsilon-\varsigma)\, X$$

$$\{Z_{os}\cosh\gamma_s\varsigma+Z_{cs}\sinh\gamma_s\varsigma\}d\varsigma$$

$$-\int_0^{\upsilon} \sinh\gamma i\,(\upsilon-\varsigma)\cosh\gamma_s(\upsilon-\zeta)\tau(\zeta)d\zeta$$

$$- \eta(\upsilon) + \eta(0)\cosh\gamma_s\upsilon\}d\upsilon \qquad (8)$$

$$\delta si(\upsilon)=- \frac{Z_T}{Z_{ci}Z_{cs}}\frac{\kappa_{ss}}{\Delta_{ss}}\int_0^{\upsilon} \sinh\gamma_i(\upsilon-\zeta)\, X$$

$$[Z_{os}\sinh\gamma_s\zeta+Z_{cs}\cosh\gamma_s\zeta]d\zeta$$

$$+\int_0^{\upsilon} \sinh\gamma_i(\upsilon-\upsilon)\, X$$

$$\{\eta(0)\sinh\gamma_s\upsilon+\sinh\gamma_s(\upsilon-\zeta)\tau(\zeta)d\zeta\}d\upsilon$$

$$-Y_T\frac{\kappa_{ss}}{\Delta_{ss}}\int_0^{\upsilon} \cosh\gamma_i(\upsilon-\zeta)\, X$$

$$\{Z_{os}\cosh\gamma_s\zeta+Z_{cs}\sinh\gamma_s\zeta\}d\zeta$$

$$+\int_0^{\upsilon}\cosh\gamma_i(\upsilon-\upsilon)\{\int_0^{\upsilon}\cosh\gamma_s(\upsilon-\zeta)\tau(\zeta)d\zeta$$

$$- \eta(\upsilon)+\eta(0)\cosh\gamma_s\upsilon\}d\upsilon \qquad (9)$$

With the Thevenin equations for the terminal conditions current and voltages inside the coaxial cable are obtained from above equations as

$$I_i(0) = \frac{\kappa_{ii}}{\Delta_{ii}}$$

$$V_i(0)=- Z_{oi}I_i(0)$$

$$I_i(L)=\left(\frac{Z_{os}}{Z_{cs}}\sinh\gamma_i L+\cosh\gamma_i L\right)\frac{\kappa_{ii}}{\Delta_{ii}}+\delta_{si}(L)$$

$$V_i(L)=-(Z_{oi}\cosh\gamma_i L+Z_{ci}\sinh\gamma_i L)\frac{\kappa_{ii}}{\Delta_{ii}}+\vartheta_{si}(L) \qquad (10)$$

where

$$\kappa_{ii}=Z_{ci}[\vartheta_{si}(L)-Z_{Li}\delta_{si}(L)]$$

$$\kappa_{ss}=Z_{cs}[\vartheta_{ss}(L)-Z_{Ls}\delta_{ss}(L)]$$

$$\Delta_{ss}=(Z_{cs}Z_{os}+Z_{cs}^2)\sinh\gamma_s L+Z_{cs}(Z_{os}+Z_{Ls})\cosh\gamma_s L$$

$$\Delta_{ii}=(Z_{ci}Z_{oi}+Z_{ci}^2)\sinh\gamma_i L+Z_{ci}(Z_{oi}+Z_{Li})\cosh\gamma_i L \qquad (11)$$

Near end (υ=0) and far end (υ=L) responses of the line are obtained from the coupled voltages $V_i(0)$ and $V_i(L)$ as given above and the coupling factor is computed from the normalised values of this vectors to the maximum value of the incident field.

The incident plane waves are considered for parallel (E-field parallel to xz-plane, as shown in Fig.2) polarisation, for which E-field may be obtained as

$$E_x^i=E_o\cos\theta\cos\phi\{e^{jk_u u}-\rho e^{-jk_u u}\}e^{-jk_\upsilon \upsilon}$$

$$E_y^i=E_o\sin\{e^{jk_u u}+\rho e^{-jk_u u}\}e^{-jk_\upsilon \upsilon} \qquad (12)$$

where E_o is the maximum field intensity, From Fig.1 the scalar wave numbers can be obtained as $k_\upsilon=(2\pi/\lambda)\sin\theta\sin\phi$, and $k_u=(2\pi/\lambda)\sin\theta\cos\phi$, ρ is the reflection coefficient for the oblique incidence on to ground plane of the incident wave and it is calculated using the expressions in [Frankel 1979].

RESULTS

In this section simulations have been carried out to investigate the response of a coaxial cable excited by an external plane wave with arbitrary polarisation and orientation with respect to cable axis. Several braid

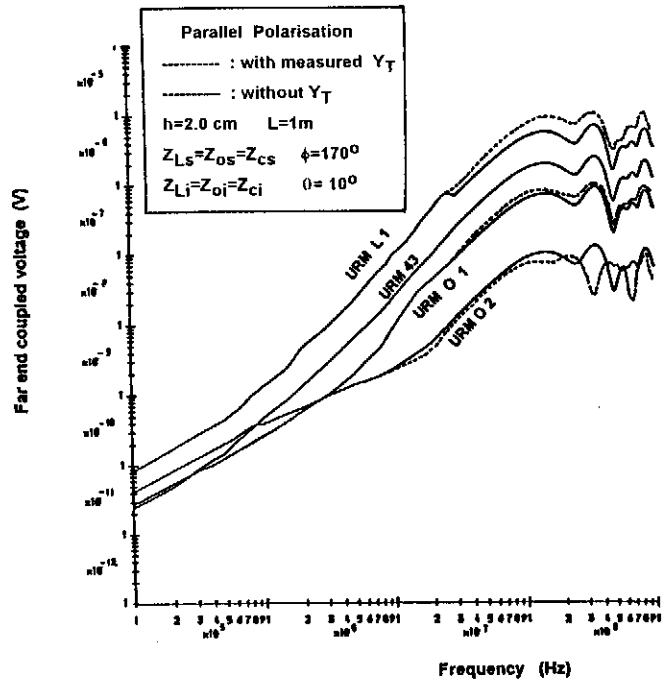

Fig.4 Frequency response of the cable samples examined. The sheath and cable matched at both ends. Results are computed by using measured values of Y_T.

designs under different load conditions in the tertiary circuit were investigated, using the standard (high optical coverage), optimised and leaky (low optical coverage) of URM43 size (2.95 mm over inner dielectric) cables. The results of these measurements are given in [Sali 1993] and [Sali 1990] and they are used in these studies also. The electrical and geometrical parameters of the cable samples used in the studies are given in Table I of the Appendix.

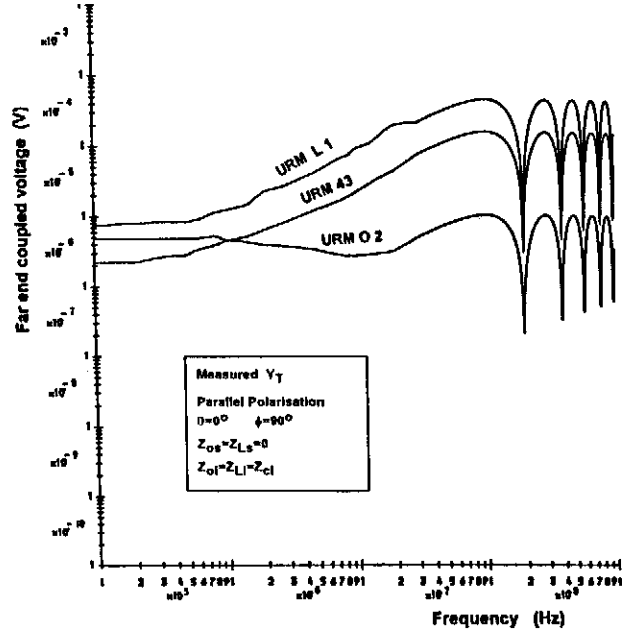

Fig.5 Frequency response for a 1m sample of URM L 1. The sheath is shorted to a conducting plane at both ends. The cable is matched. Results are computed using measured values of Y_T in the general method.

A general computer program was developed using the theoretical field coupling model in Section II. The frequency range was between 100 KHz and 1 GHz. In each case the incident field was a uniform plane wave with a maximum E-field intensity of 1V/m, and the conducting plane was assumed to be made of Aluminium. Since all the existing EMI studies on braid wire shielded cables ignore Electric field coupling no comparable study exists in the literature. However the accuracy of our EMI model is checked against the technique suggested in [Smith 1977]. Since Smith's model, is originally suggested for lossless shield above lossless conducting plane and ignores Y_T coupling our model had to be simplified to this simple case before the comparison. Results of these studies showed that both approaches produce identical results.

Fig.4 shows the results for the far end induced voltage for URM43 (standard), URM L 1 (leaky) , URM O 1 ,and URM O 2 (both optimised) cables respectively, when the tertiary circuit and the interior of the cables are matched. Graphs with solid lines show the responses of the cables when Y_T is returned zero in the interference model and those with broken lines show the results for the same cables when the measured values of Y_T are included in the calculations . The results for URM 43 (which has a high optical coverage and Z_T values) show that coupling curves with and without Y_T are almost identical. However curves for URM O 2 and L 1 give 20 dB difference in the standing wave region with and without Y_T included in the model. Fig.5 shows the results when external circuit is shorted to the conducting plane. The short circuits enhance the series magnetic currents in the tertiary at the expense of shunt voltages between the shield and the conducting plane. In this case the magnetic field coupling dominates. Further simulations have already confirmed that coupling curves with and without Y_T are almost identical for all cable samples with shorted external circuit and the electric field coupling may be ignored .

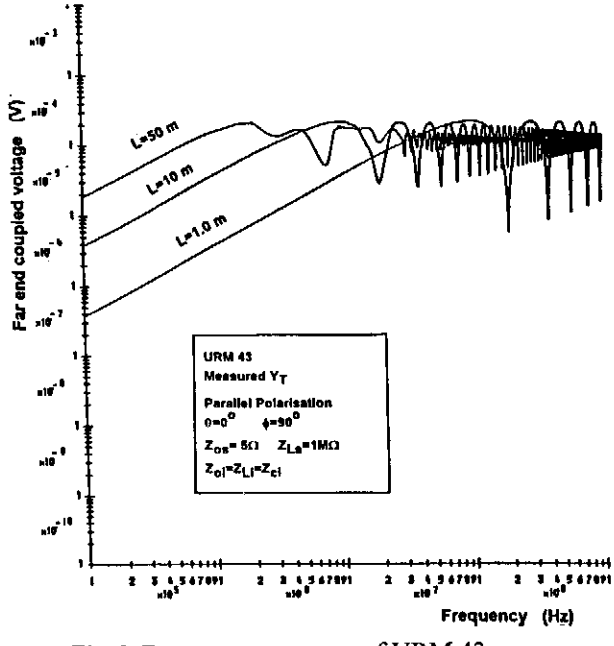

Fig.6 Frequency response of URM 43 versus coupling length.

The amount of energy coupled to the cable depends on the amount of flux induced by the dipole (or scattered) mode fields in the area between the braided shield and the ground plane, as illustrated in Fig.3. Simulations have been carried out to investigate the effect of increased surface area on the amount of the field coupling to inside of the cable, by simply varying either the length or the height of the shield from the ground plane.Fig.6 shows the results for the far -end coupled voltage against frequency when the length of the cable is varied between 1.0 m and 50.0 m. It is seen that increased length results in much higher coupling levels at low frequencies but no noticeable difference between the amplitude values is observed at high frequencies because of the increased attenuation which cancels the increased coupling levels at such frequencies. However the standing wave pattern is brought down to much lower frequencies when the length is increased, as expected. Further simulations have been carried out to investigate the variation of the coupled voltage when the height of the cable is varied from 0.5 mm to 5.0 cm and the results are shown in Fig.7 in the frequency domain. Increase in the coupled voltage is quite rapid at the initial stages but slows down gradually, and little increase is observed for heights greater than 7.0 cm.

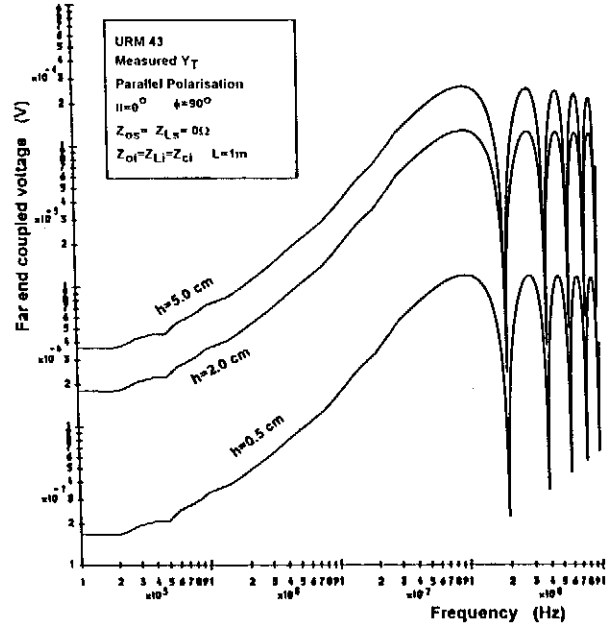

Fig.7 Frequency response for 1m sample of URM 43 cable versus height from the ground plane.

The effect of the cable height on the coupling power is further studied in Fig.8, which shows the coupled voltage induced from a 300 MHz plane wave along the cable length. Note that a coupling minima is expected to occur at 0.5m along the cable (the position here is slightly less as the velocity is taken as $c=3x10^8$). This translates to a position at around 150MHz in frequency domain which is exactly the same frequency position given by the coupling

curves in Fig.5. Results in Fig.6 to 8 clearly illustrate the spatial and frequency dependence of field coupling. Theoretically the positions of minimas are given by $L_n=n\pi/k_0$, as confirmed by these results.

Finally the angular dependence of the field coupling is studied in Figs. 9 and 10 where results for the far end coupled voltage are shown when elevation angle is fixed and azimuth angle is varied as in Fig. 9. and azimuth angle is fixed and elevation angle is varied , as in Fig.10 Bear in mind that when the fixed angles were changed in both cases, different coupling results would be obtained. This clearly illustrates that there is a strong dependence between the angular orientation of the cable with respect to the direction of Poynting vector of the incident field.

CONCLUSIONS

A general algorithm is presented for the study for the response of coaxial cables with wire braided shields excited by external electromagnetic fields. The model includes both electric and magnetic coupling parameters in contrast to the existing studies on similar problem which only include magnetic field coupling. Numerical studies using this algorithm is concentrated on coupling of the external fields to the cable with various braid designs in their shields and different load conditions in the tertiary circuits between the shield and the ground plane. The studies have covered in detail the role of field orientation and geometry of the external tertiary circuit on the amount of energy coupled to the interior of the coax. The results show that at low frequencies the electric field coupling can be ignored but this is not so at high frequencies and accurate computation of the external field coupling requires that both coupling parameters must be included in the model for optimised cables. Even with short circuited tertiaries, the electric field coupling may contribute significantly to the overall response of the cable when optimised cables are used.

REFERENCES

[Bayindir and Sali, 1990] S.A. Bayindir and S Sali, " Radiation losses in microwave integrated circuits at micro and mm-wave frequencies", Proc. of 16'th QMC Ant. Symp., University of London, 1990.

[Sali, 1993] S. Sali, " Coupling of electromagnetic fields to coplanar striplines with discontinuities", IEE Proc. Pt.H, pp.481-487, Dec.1993.

[Sali, 1993] S. Sali, " A circuit based approach for crosstalk between coaxial cables with optimum braided shields", IEE Trans. EMC-35, No.2, May 1993 pp.300-311.

[Vance, 1973] E.F. Vance, "Comparison of electric and magnetic coupling through braided wire shields", Techn. Rep. No. AFWL-TR-73, 71 Stanford Research Inst., May 1973.

[Sali , 1992] S. Sali, "Screening efficiency of triaxial cables with optimum braided shields," IEEE Trans. EMC-32, May 1992, No.4, pp.123-134.

[Fowler, 1979] E.P. Fowler, "Super screened cables," The radio and Electronic Engineer, Vol.49, No.1, April 1979, pp.38-44.

[Tyni, 1976] M. Tyni, "Transfer impedance of coaxial cables with braided outer conductors", Pr. Nauk. Inst. Telekamun. X, Aukust, Politech Wrocklow, 27, Ser, Korf 1976, pp. 410-419.

[Frankel 1977] S. Frankel," Multiconductor transmission line analysis, Artech House Inc., 1977.

[Smith 1977] A.A Smith, Jr., "Coupling of electromagnetic fields to transmission lines", J. Willey & Sons Inc., NY 1977.

[Taylor and Younan, 1992] C.D. Taylor, and N.H. Younan," Effects of high power microwave illumination", Microwave Journal, June 1992, pp.80-96.

[Harrison ,1972] C.W. Harrison, Jr., "Generalised theory of impedance loaded multiconductor transmission lines in an incident field", IEEE Trans. Vol. EMC-14, No.2, May 1972, pp.56-63.

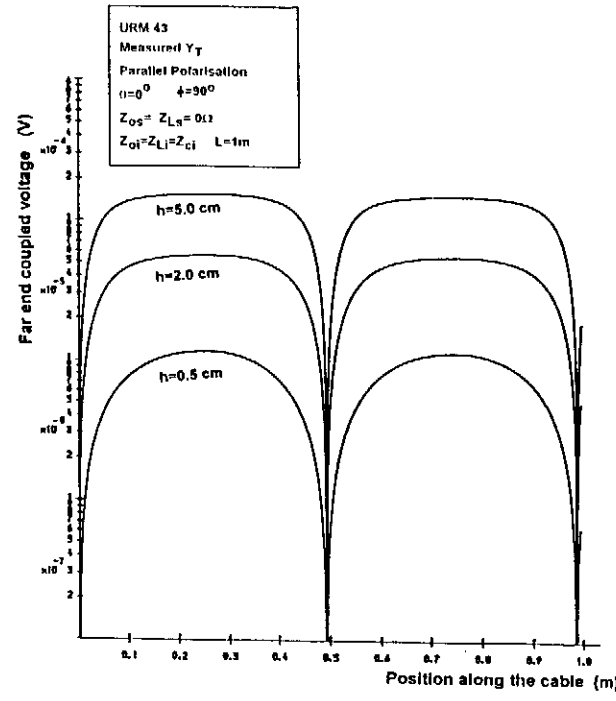

Fig.8 Response for a 1m sample of URM 43 cable versus height from the ground plane. The incident field is a 300 MHz plane wave with parallel polarization.

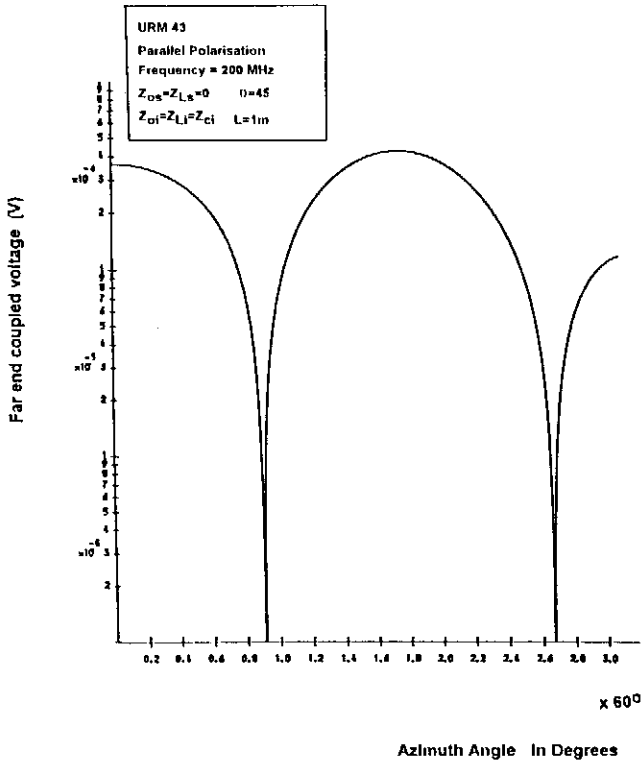

Fig.9 Response of the cable versus incident angle at elevation. Azimuth angle is fixed at ϕ=45°. Frequency of the incident wave is 200 MHz.

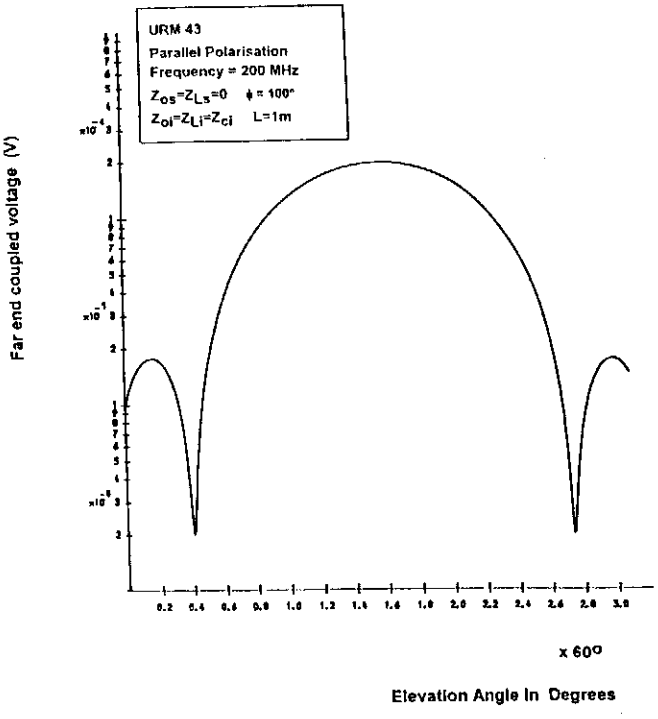

Fig.10 Response of the cable versus incidence angle at elevation. Azimuth angle is fixed at ϕ=100°. Frequency of the incident wave is 200 MHz.

APPENDIX

CABLE	M	n	DOD (mm)	BWD (mm)	LL (mm)	K_f	θ (Deg)	POL
URM 43	16	6	2.95	0.150	22.0	0.77	24.9	-
URM O 1	16	6	2.95	0.100	23.0	0.520	23.28	+
URM O 2	16	7	2.95	0.096	23.2	0.584	23.26	-
URM L 1	16	3	2.95	0.15	16.0	0.40	23.1	-

Table 1 - Geometrical parameters of the cable samples

DOD : **Diameter over inner dielectric (do)**

BWD : **Braid wire diameter (dw)**

LL : **Lay Length (l)**

θ : **Braid angle (θ) = $\tan^{-1}(\pi (do + 2.25dw)/l)$**

N : **Number of spindles**

n : **Number of braid wires per spindle**

K_f : **Filling factor K_f = Nndw/2 l sinθ**

POL : **Polarity of the transfer impedance (positive polarity indicates the dominance of the hole inductance and negative polarity that of braid inductance)**

CABLE SAMPLES